Associative Ligand Substitution Reactions of Low-Valent Rhenium-Oxo Compounds. Crystal and Molecular Structures of $[ReO(MeC{\equiv}CMe)_2L]SbF_6$, L = Pyridine and 4,4′-Dimethyl-2,2′-bipyridine

James M. Mayer,*† T. H. Tulip,‡§ J. C. Calabrese,‡ and Esther Valencia†

Contribution from the Department of Chemistry, The University of Washington, Seattle, Washington 98195, and Central Research and Development Department, E. I. du Pont de Nemours and Company, Inc.,‡ Experimental Station, Wilmington, Delaware 19898.
Received June 2, 1986

Abstract: A series of rhenium-oxo compounds of the form $[ReO(RC{\equiv}CR')_2L]SbF_6$ have been prepared where L is a substituted pyridine or bipyridine ligand. Structures have been determined by X-ray crystallography for $[ReO(MeC{\equiv}CMe)_2(NC_5H_5)]SbF_6$ (**2**) and $[ReO(MeC{\equiv}CMe)_2(4,4'\text{-}Me_2\text{-}2,2'\text{-}bpy)]SbF_6$ (**7**); both molecules contain a short multiple rhenium-oxygen bond of 1.692 (3) Å. The coordination geometry in **2** can be described as a slightly distorted tetrahedron in which each of the acetylene ligands occupies one vertex. In contrast the structure of **7** does not closely resemble any idealized five-coordinate geometry; it resembles the structure of **2** with the pyridine ligand replaced by a bidentate bipyridine ligand. The complexes of pyridine and 4-substituted pyridines undergo a very facile ligand-exchange reaction with free ligand in solution, but complexes of 2-substituted pyridines are much more inert. NMR studies indicate that the substitution reactions proceed with retention of stereochemistry, by an associative mechanism involving front-side attack at the tetrahedral rhenium center. The five-coordinate intermediate or transition state formed probably closely resembles the structure of **7**. The long rhenium-nitrogen distances in **7** are consistent with this view (Re-N = 2.246, 2.337 (4) Å; compare **2**, Re-N = 2.118 (3) Å). The unusual preference for retention of configuration derives from the electronic influence of the rhenium-oxygen multiple bond. The rhenium-pyridine complexes are best described as 18-electron, coordinately saturated species; the ligand-exchange reactions are therefore similar to S_N2 reactions at saturated carbon centers, except for the difference in stereochemistry. Crystallographic data for **2**: space group $P\bar{1}$, a = 10.482 (1) Å, b = 12.117 (2) Å, c = 7.880 (1) Å, α = 105.34 (1)°, β = 108.03 (1)°, γ = 99.05 (1)°, Z = 2, refined to R = 0.020, R_w = 0.027. Data for **7**: space group $P2_1/c$, a = 7.872 (1) Å, b = 21.735 (3) Å, c = 13.492 (2) Å, β = 100.70 (1)°, Z = 4, refined to R = 0.026, R_w = 0.028.

Mechanisms of substitution reactions have been an active area of research since Ingold's 1933 proposal of S_N1 and S_N2 mechanisms for substitution at carbon centers.[1] The substitution chemistry of transition-metal compounds is complicated by the variety of coordination geometries and electronic structures known for transition-metal species.[2] The critical role of d electron configuration in the reactions of octahedral metal complexes was first described by Taube in 1952.[3] As an example, the rate of exchange of water molecules in $M(H_2O)_6^{3+}$ with the solvent is 10^9 times faster for $Fe(H_2O)_6^{3+}$ than for $Cr(H_2O)_6^{3+}$.[4] Different electronic factors are important in organometallic substitution reactions: 18-electron compounds usually exchange ligands by dissociative mechanisms while 16-electron species often react associatively.[5]

We wish to report a facile ligand-exchange reaction involving tetrahedral rhenium complexes. The exchange occurs by an associative mechanism, with retention of configuration at rhenium. This contrasts with associative substitution at tetrahedral carbon centers (S_N2 processes), which proceed with inversion of configuration at carbon.

Tetrahedral transition-metal complexes are usually labile in solution because those with partially filled d shells almost always have "high-spin" electronic configurations.[6,7] Our recently reported rhenium oxo-acetylene complexes are rare examples of low-spin tetrahedral species.[8] A molecular orbital analysis indicated that the unusual electronic configuration and structure are due to the presence of a terminal, multiply bonded oxo ligand in the relatively low-valent complexes.[8] Terminal oxo ligands had previously only been observed in high-valent metal compounds.[8,9] The electronic requirements of the Re(III)-oxygen multiple bond not only determine the geometry of these molecules but also dictate the stereochemistry of their ligand-exchange reactions.

Results

A number of pyridine derivatives of the form $[ReO(MeC{\equiv}CMe)_2L]SbF_6$ have been prepared following the procedure previously described for **2** and **6** (eq 1).[8,10] Compounds containing

$$\underset{\mathbf{1}}{Re(O)I(MeC{\equiv}CMe)_2} + AgSbF_6 + L \rightarrow [ReO(MeC{\equiv}CMe)_2L]SbF_6 + AgI \quad (1)$$

2, L = py
3, L = 4-Mepy
4, L = 2-Mepy
5, L = 2,6-Me_2py
6, L = bpy
7, L = 4,4′-Me_2bpy

acetylenes other than 2-butyne have also been prepared (eq 2-4).

† University of Washington.
‡ Du Pont Company, Contribution No. 3844.
§ Present address: Biomedical Products Department, E. I. du Pont de Nemours and Co. N. Billerica, MA 01862.

(1) Lowry, T. H.; Richardson, K. S. *Mechanism and Theory in Organic Chemistry*; Harper and Row: New York, 1976; pp 170-209 and references therein.
(2) (a) Langford, C. H.; Gray, H. B. *Ligand Substitution Reactions*; W. A. Benjamin: New York, 1965. (b) Basolo, F.; Pearson, R. G. *Mechanisms of Inorganic Reactions*, 2nd ed.; Wiley: New York, 1967.
(3) Taube, H. *Chem. Rev.* **1952**, *50*, 69-126.
(4) Reference 2b, p 152.
(5) Tolman, C. A. *Chem. Soc. Rev.* **1972**, *1*, 337-353.
(6) Cotton, F. A.; Wilkinson, G. *Advanced Inorganic Chemistry*, 4th ed.; Wiley: New York, 1980; p 647.
(7) The recently reported OsR_4 compounds are remarkable examples of apparently low-spin tetrahedral species: Tooze, R. P.; Stavropolous, P.; Motevalli, M.; Hursthouse, M. B.; Wilkinson, G. *J. Chem. Soc., Chem. Commun.* **1985**, 1139-1140.
(8) Mayer, J. M.; Tulip, T. H. *J. Am. Chem. Soc.* **1984**, *106*, 3878-3879. Mayer, J. M.; Thorn, D. L.; Tulip, T. H. *J. Am. Chem. Soc.* 1985, *107*, 7454.
(9) (a) Griffith, W. P. *Coord. Chem. Rev.* **1970**, *5*, 459-517. (b) Gulliver, D. J.; Levason, W. *Coord. Chem. Rev.* **1982**, *46*, 1-127. (c) Reference 6.
(10) Abbreviations: py, pyridine (C_5H_5N); 2- or 4-Mepy, 2- or 4-methylpyridine (2- or 4-picoline); 2,6-Me_2py, 2,6-dimethylpyridine (2,6-lutidine); 2- or 4-Etpy, 2- or 4-ethylpyridine; bpy, 2,2-bipyridine; 4,4′-Me_2bpy, 4,4′-dimethyl-2,2′-bipyridine; and THF, tetrahydrofuran.

0002-7863/87/1509-0157$01.50/0

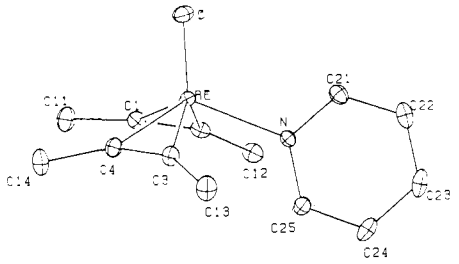

Figure 1. Perspective drawing of $[ReO(MeC{\equiv}CMe)_2py]^+$ (**2**). Hydrogen atoms have been omitted for clarity. Vibrational ellipsoids are drawn at the 50% probability level.

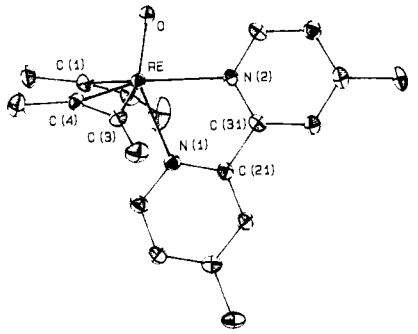

Figure 2. Perspective drawing of $[ReO(MeC{\equiv}CMe)_2(Me_2bpy)]^+$ (**7**). Hydrogen atoms have been omitted for clarity. Vibrational ellipsoids are drawn at the 50% probability level.

These materials are off-white crystalline solids, diamagnetic, and soluble in polar solvents such as methylene chloride or THF.

$$Re(O)I(Me_3CC{\equiv}CH)_2 + AgSbF_6 + L \rightarrow [ReO(Me_3CC{\equiv}CH)_2L]SbF_6 + AgI \quad (2)$$

8, L = py
9, L = 4-Etpy
10, L = 2-Etpy

$$Re(O)I(MeC{\equiv}CPh)_2 + AgSbF_6 + py \rightarrow [ReO(MeC{\equiv}CPh)_2py]SbF_6 + AgI \quad (3)$$

11

$$Re(O)I(EtC{\equiv}CEt)_2 + AgSbF_6 + 4\text{-Mepy} \rightarrow [ReO(EtC{\equiv}CEt)_2(4\text{-Mepy})]SbF_6 + AgI \quad (4)$$

12

The X-ray crystal structures of **2** and **7** both contain discrete rhenium cations and SbF_6 anions (Figures 1 and 2). Fractional atomic coordinates are listed in Tables I and II. Bond distances and angles for **2** and **7** appear in Table III together with data for the related complex $Re(O)I(MeC{\equiv}CMe)_2$, **1**.[8] Complexes **1**, **2**, and **7** have close to C_s symmetry in the solid state with the mirror plane containing the Re–O bond and relating the two acetylenes in the $ReO(MeC{\equiv}CMe)_2$ fragment. This fragment is remarkably similar in the three structures. For instance, in all three the rhenium–oxygen bond axis is close to perpendicular to the plane defined by the four acetylenic carbon atoms: the angles between the ReO vector and the normal to the C(1,2,3,4) plane are 9.3° (**1**), 9.0° (**2**), and 10.4° (**7**). The rhenium–oxygen distances are the same within experimental error (1.692–1.697(3) Å) and are typical of Re–O multiple bonds.[8]

In compound **2**, as in **1**, the six atoms bound to the rhenium center roughly describe a pentagonal pyramid with the oxygen atom at the apex. There are close nonbonded contacts among the acetylenic carbon atoms and the nitrogen atom that comprise the pentagonal plane: N···C(2) = 2.768 (5), N···C(3) = 2.747 (5), and C(1)···C(4) = 2.874 (6) Å (the van der Waals radii of carbon and nitrogen are roughly 1.7 and 1.55 Å[11]). The close nonbonded contact between C(1) and C(4) is found in all three structures. The coordination geometries of **1** and **2** are probably best thought of as tetrahedral with the acetylene midpoints occupying two vertices. In this description all of the bond angles about rhenium are within 9° of the tetrahedral angle.

(11) Huheey, J. E. *Inorganic Chemistry*, 3rd ed.; Harper and Row: New York, 1983; p 258.

Table I. Fractional Atomic Coordinates and Isotropic Thermal Parameters[a] for $[ReO(MeC{\equiv}CMe)_2py]SbF_6$ (**2**)

atom	x	y	z	B, Å²
Re	0.1632 (1)	0.1905 (1)	0.1692 (2)	1.393 (4)
Sb	0.6533 (3)	0.3044 (2)	0.0638 (4)	2.00 (1)
O	0.6403 (6)	0.2571 (6)	−0.1883 (7)	5.0 (2)
N	0.5971 (29)	0.2064 (21)	−0.1714 (36)	6.3 (9)
F(1)	0.4700 (3)	0.3146 (3)	−0.0056 (5)	4.3 (1)
F(2)	0.8348 (3)	0.2888 (4)	0.1338 (5)	5.1 (1)
C(3)	0.6372 (23)	0.1910 (17)	0.1683 (30)	5.6 (8)
F(3)	0.6634 (5)	0.3420 (5)	0.3133 (5)	4.7 (2)
F(4)	0.7260 (18)	0.4217 (19)	0.3079 (22)	4.8 (6)
C(4)	0.5893 (5)	0.1431 (3)	0.0357 (8)	4.8 (2)
F(5)	0.7146 (6)	0.4599 (4)	0.0928 (10)	6.1 (2)
F(6)	0.6760 (28)	0.4349 (22)	−0.0234 (32)	6.6 (9)
C(14)	0.0511 (3)	0.1112 (3)	0.2354 (4)	2.4 (1)
C(13)	0.0673 (3)	0.2198 (3)	−0.0883 (4)	1.5 (1)
C(1)	0.2919 (4)	0.3363 (3)	0.3918 (5)	2.0 (1)
C(2)	0.2002 (4)	0.3711 (3)	0.2818 (5)	1.9 (1)
F(3′)	−0.1388 (5)	0.1796 (4)	−0.3557 (6)	2.9 (1)
F(4′)	−0.0690 (5)	0.2462 (4)	−0.4301 (6)	2.9 (1)
F(5′)	0.0714 (5)	0.3020 (4)	−0.3301 (6)	2.8 (1)
F(6′)	0.1369 (4)	0.2873 (4)	−0.1600 (6)	2.2 (1)
C(11)	0.4168 (5)	0.3725 (4)	0.5670 (6)	3.0 (1)
C(12)	0.1500 (5)	0.4739 (4)	0.2440 (7)	2.9 (1)
C(21)	0.3252 (4)	0.1148 (3)	0.1886 (6)	1.9 (1)
C(22)	0.2564 (4)	0.0930 (3)	0.0122 (6)	1.8 (1)
C(23)	0.4429 (5)	0.0985 (4)	0.3344 (6)	2.8 (1)
C(24)	0.2474 (4)	0.0406 (4)	−0.1841 (6)	2.4 (1)
C(25)	−0.0685 (4)	0.1673 (4)	−0.1850 (6)	2.2 (1)

[a] Anisotropically refined atoms are given in the form of the isotropic equivalent thermal parameter defined as $\exp[-19.739(U_{11}h^2a^{*2}... + 2(U_{12}hka^*b^* + ...))]$.

Table II. Fractional Atomic Coordinates and Isotropic Thermal Parameters[a] for $[ReO(MeC{\equiv}CMe)_2(4,4'\text{-}Me_2bpy)]SbF_6$ (**7**)

atom	x	y	z	B, Å²
Re	0.58758 (3)	0.43926 (1)	0.31241 (2)	1.262 (3)
Sb	0.09844 (6)	0.68144 (2)	0.24878 (4)	2.314 (8)
F(1)	0.2837 (6)	0.7273 (2)	0.2210 (4)	4.3 (1)
F(2)	−0.0031 (7)	0.7530 (2)	0.2855 (4)	4.9 (1)
F(3)	−0.0114 (7)	0.6935 (2)	0.1152 (4)	4.9 (1)
F(4)	0.2015 (7)	0.6102 (2)	0.2113 (5)	5.6 (1)
F(5)	0.2168 (9)	0.6693 (3)	0.3809 (4)	6.5 (2)
F(6)	−0.0820 (7)	0.6339 (3)	0.2758 (5)	6.7 (1)
O	0.3994 (5)	0.4131 (2)	0.3401 (3)	1.77 (8)
N(1)	0.7872 (5)	0.4357 (2)	0.2132 (3)	1.39 (8)
N(2)	0.5287 (6)	0.3601 (2)	0.1937 (4)	1.40 (9)
C(1)	0.7529 (7)	0.4423 (3)	0.4491 (4)	1.7 (1)
C(2)	0.7957 (8)	0.3958 (3)	0.4019 (5)	1.9 (1)
C(3)	0.5413 (7)	0.5191 (3)	0.2290 (5)	1.6 (1)
C(4)	0.5737 (7)	0.5329 (3)	0.3225 (4)	1.6 (1)
C(11)	0.7985 (9)	0.4784 (3)	0.5437 (5)	2.1 (1)
C(12)	0.926 (1)	0.3455 (3)	0.4016 (6)	3.4 (2)
C(13)	0.5182 (9)	0.5478 (3)	0.1267 (5)	2.4 (1)
C(14)	0.6042 (9)	0.5878 (3)	0.3924 (5)	2.4 (1)
C(21)	0.7817 (7)	0.3943 (3)	0.1379 (4)	1.4 (1)
C(22)	0.9085 (7)	0.3915 (3)	0.0802 (4)	1.6 (1)
C(23)	1.0475 (7)	0.4322 (3)	0.0978 (4)	1.6 (1)
C(24)	1.0547 (8)	0.4740 (3)	0.1763 (5)	1.9 (1)
C(25)	0.9218 (8)	0.4752 (3)	0.2312 (5)	1.9 (1)
C(26)	1.1826 (7)	0.4317 (3)	0.0322 (5)	2.1 (1)
C(31)	0.6304 (7)	0.3533 (3)	0.1243 (4)	1.4 (1)
C(32)	0.5952 (8)	0.3101 (3)	0.0461 (4)	1.6 (1)
C(33)	0.4508 (8)	0.2728 (3)	0.0391 (5)	1.9 (1)
C(34)	0.3462 (8)	0.2795 (3)	0.1120 (5)	1.8 (1)
C(35)	0.3894 (7)	0.3232 (3)	0.1876 (5)	1.6 (1)
C(36)	0.4076 (9)	0.2268 (3)	−0.0461 (5)	2.7 (1)

[a] Anisotropically refined atoms are given in the form of the isotropic equivalent thermal parameter defined as $^4/_3\,[a^2B_{11} + b^2B_{22} + c^2B_{33} + ab(\cos\gamma)B_{12} + ac(\cos\beta)B_{13} + bc(\cos\alpha)B_{23}]$.

Table III. Comparison of Selected Bond Distances (Å) and Angles (deg) in $Re(O)I(MeC{\equiv}CMe)_2$ (**1**), $[ReO(MeC{\equiv}CMe)_2py]SbF_6$ (**2**), and $[ReO(MeC{\equiv}CMe)_2(Me_2bpy)]SbF_6$ (**7**)

	1[a,b]	**2**	**7**
	Distances		
Re-O	1.697 (3)	1.692 (3)	1.692 (3)
Re-N(1)	2.691 (1)[b]	2.118 (3)	2.246 (3)
Re-N(2)			2.337 (4)
Re-C(1)	2.038 (5)	2.041 (4)	2.052 (4)
Re-C(2)	2.061 (5)	2.054 (4)	2.074 (4)
Re-C(3)	2.066 (5)	2.054 (4)	2.063 (4)
Re-C(4)	2.040 (5)	2.038 (4)	2.045 (4)
C(1)-C(2)	1.278 (7)	1.288 (6)	1.273 (6)
C(3)-C(4)	1.288 (7)	1.283 (6)	1.276 (6)
	Angles		
O-Re-N(1)	109.4 (1)[b]	113.8 (1)	149.1 (1)
O-Re-N(2)			80.4 (1)
O-Re-C(1)	109.1 (2)	110.6 (1)	104.3 (2)
O-Re-C(2)	114.8 (2)	114.6 (1)	110.3 (2)
O-Re-C(3)	114.1 (2)	115.3 (1)	109.2 (2)
O-Re-C(4)	108.8 (2)	106.9 (1)	105.1 (2)
N(1)-Re-C(1)	119.6 (2)[b]	116.2 (1)	98.0 (1)
N(1)-Re-C(2)	85.2 (1)[b]	83.1 (1)	76.5 (2)
N(1)-Re-C(3)	85.2 (1)[b]	82.4 (1)	77.1 (2)
N(1)-Re-C(4)	119.7 (2)[b]	117.2 (1)	97.2 (2)
N(2)-Re-C(1)			130.7 (2)
N(2)-Re-C(2)			95.7 (2)
N(2)-Re-C(3)			104.6 (2)
N(2)-Re-C(4)			140.5 (2)
N(1)-Re-N(2)			68.8 (1)
C(1)-Re-C(2)	36.3 (2)	36.7 (2)	35.9 (2)
C(1)-Re-C(3)	117.6 (2)	116.1 (2)	118.8 (2)
C(1)-Re-C(4)	88.3 (2)	89.6 (2)	86.6 (2)
C(2)-Re-C(3)	130.5 (2)	129.7 (1)	137.9 (2)
C(2)-Re-C(4)	117.3 (2)	120.1 (2)	117.5 (2)
C(3)-Re-C(4)	36.6 (2)	36.6 (2)	36.2 (2)
Re-C(1)-C(11)[c]	141.3 (4)	141.7 (3)	143.3 (4)
C(1)-C(2)-C(12)[c]	144.3 (5)	146.5 (4)	145.6 (5)

[a] Data from ref 8. [b] Bond distance or angle involves the iodide ligand, not N(1). [c] Related bond angles have very similar values (±4°).

The structure of the bipyridine complex **7**, on the other hand, does not closely resemble any idealized five-coordinate geometry. The rhenium–oxygen bond is coplanar with the bipyridine ligand, suggesting a very distorted trigonal-bipyramidal structure, but there is no true trans ligand (O-Re-N(1) = 149.1 (1)°), and the oxygen–rhenium–acetylene midpoint angles (av 112°) are much larger than 90° while the O-Re-N(2) angle is smaller (80.4 (1)°). Since the $ReO(MeC{\equiv}CMe)_2$ fragment is essentially identical with that in **1** and **2**, the coordination geometry of **7** could be described as a tetrahedron in which the bipyridine ligand occupies only one site. Consistent with this description, the position of the pyridine ligand in **2** bisects the N(1)-Re-N(2) angle in **7**.

The structure of **7** is unusual not only in its irregular coordination geometry but also in the very long rhenium–nitrogen bonds (2.246 (3) and 2.337 (4) Å), which are substantially longer than the Re-N distance in **2** of 2.118 (3) Å. Previously reported rhenium–pyridine distances range from 2.116 (16) to 2.245 (8) Å.[12] The shorter rhenium–nitrogen bond in **7** is the one pseudo-trans to the oxygen, which is surprising in view of the high trans influence of an oxo ligand.[13,14] The large difference between the two Re-N distances in **7** (0.09 Å) may be due to repulsion between the oxo and bipyridine ligands (O···H(C(35)) = 2.35, O···N(2) = 2.65 Å). These short contacts are a consequence of the small O-Re-N(2) angle (80°) and do not appear to be balanced by steric crowding at the other end of the bipyridine ligand (N(1)···C(2) = 3.13 Å). This suggests that the unusual O-Re-N bond angles are due to an electronic preference rather than steric constraints. The structure of **7** appears to be maintained in solution, since the IR spectra for solid and dissolved **7** are similar.[15] A comparison of **7** with **2** suggests that the addition of a second pyridine ligand results in a slight weakening of the rhenium–acetylene bonding since there is a small increase in Re-C distances (av 0.012 Å) and a small decrease in acetylenic C-C bond distances (av 0.011 Å), although these differences are at the edge of statistical significance.

The NMR and IR spectra of **2** and **7** are consistent with solution structures which are analogous to the observed solid-state structures. For instance, the proton NMR spectrum of **2** contains two resonances due to the 2-butyne ligands, one corresponding to the two methyl groups adjacent to the pyridine ligand, the other to the two distant methyl groups. Compounds **3–5** and **8–12** have NMR and IR spectra similar to those of **2** and are therefore assumed to adopt the same basic structure. The NMR spectra of **2–5** and **8–12**, like those of **1**,[8] indicate that the acetylene ligands do not rotate on the NMR time scale at ambient temperatures. The five-coordinate compounds **6** and **7** are also not fluxional, with non-rotating acetylene ligands and inequivalent ends of the bipyridine ligands. Compounds **3**, **4**, and **7** have been shown to be rigid on the NMR time scale at 70 °C.

Addition of pyridine to a solution of **2** causes little change in the ^1H NMR resonances for the 2-butyne ligands, but the pyridine resonances shift and increase in intensity. Only one set of resonances is observed for both bound and free pyridine in the presence of excess pyridine. This implies that exchange between bound and free pyridine is occurring and that the exchange is fast relative to the NMR time scale. Similar results indicate that rapid ligand exchange also occurs in **3**, **8**, **9**, **11**, and **12**. The exchange process is facile even at low temperatures: solutions of **3** and 4-methylpyridine in CD_2Cl_2 at −95 °C show only a single NMR resonance due to the pyridine methyl group.

In contrast, NMR studies of **4–7** and **10**, which contain pyridine ligands substituted at the 2-position, show that ligand exchange is slow relative to the NMR time scale at ambient temperatures. The signals for free and bound 2-methylpyridine in **4** coalesce at elevated temperatures, corresponding to a bimolecular rate constant of 5×10^3 M^{-1} s^{-1} at 60 °C (see Experimental Section). This is much slower than the exchange of **2** with 4-methylpyridine, for which $k > 10^3$ M^{-1} s^{-1} at −90 °C. The steric bulk of both the entering and leaving groups is important: while degenerate exchange of 2-substituted pyridines is slow, exchange of a 2-substituted pyridine ligand with unsubstituted pyridine occurs on the NMR time scale at 25 °C. Thus the exchange of bound and free 2-methylpyridine can be catalyzed by pyridine, presumably by pyridine displacing bound 2-methylpyridine and then itself being displaced.

The substantial rate difference between the 2- and 4-substituted pyridine-exchange reactions indicates that the substitution proceeds by an associative (A or Ia) mechanism.[2] While 2- and 4-sub-

(12) Drew, M. G. B.; Davis, K. M.; Edwards, D. A.; Marshalsea, J. *J. Chem. Soc., Dalton Trans.* **1978**, 1098. Sergienko, V. S.; Khodashova, T. S.; Porai-Koshits, M. A.; Butman, L. A. *Koord. Khim.* **1977**, *3*, 1060. Ciani, G.; Giusto, D.; Manassero, M.; Sansoni, M. *J. Chem. Soc., Dalton Trans.* **1978**, 798. Horn, E.; Snow, M. R. *Aust. J. Chem.* **1980**, *33*, 2369. Lock, C. J. L.; Turner, G. *Can. J. Chem.* **1977**, *55*, 333; **1978**, *56*, 179. Lock, C. J. L.; Turner, G. *Acta Crystallogr., Sect. B: Struct. Crystallogr. Cryst. Chem.* **1978**, *34B*, 923.

(13) Kokunov, Yu. V.; Buslaev, Yu. A. *Coord. Chem. Rev.* **1982**, *47*, 15–40. Stiefel, E. I. *Prog. Inorg. Chem.* **1977**, *22*, 1–223. Rouschias, G. *Chem. Rev.* **1974**, *74*, 531–566. Dori, Z. *Prog. Inorg. Chem.* **1981**, *28*, 239–307. References 10 and 11 in ref 8. Bright, D.; Ibers, J. A. *Inorg. Chem.* **1969**, *8*, 709–716. The relevance of a trans influence in **7**, where the O-Re-N(2) angle is 149°, is questionable.

(14) Comparison of **2** and **7** with the nitride complexes $Mo(N)(N_3)_3L$, L = py (A) and bpy (B), is helpful. A has a square-pyramidal structure with no ligand trans to the nitride ligand, while B has a distorted octahedral structure with one end of the bpy ligand in the trans position. Unlike **7**, the structure of B is as expected: one of the rings of the bpy ligand in B is in a position very similar to that of the pyridine ligand in A, and the bond trans to the π donor nitride in B is much longer than the cis bonds in A or B. A: Mo-py = 2.258 (3) Å, $\angle N^{3-}$-Mo-py = 94.0 (1)°. B: Mo-N(bpy, cis to N^{3-}) = 2.240 (5) Å, Mo-N(bpy, trans) = 2.419 (5) Å, $\angle N^{3-}$-Mo-bpy = 92.0°, 161.5 (2)°. Schweda, E.; Strahle, J. *Z. Naturforsch. B: Anorg. Chem., Org. Chem.* **1980**, *35B*, 1146; **1981**, *36B*, 662.

(15) The only significant difference between the IR spectra of a Nujol mull of **7** and a solution in CH_2Cl_2 is a 6-cm^{-1} shift of the Re-O stretching mode, from 955 to 961 cm^{-1}. For comparison, ν(Re-O) = 973, 975 cm^{-1} for **3** (solid, solution). Thus we believe that both nitrogen atoms in **7** are bound to rhenium in solution, as in the solid. (See also the Discussion section and ref 23.)

stituted pyridines are electronically similar, the former are much more sterically demanding ligands. Steric hindrance should favor dissociative processes, but there is no evidence for ligand loss even in the most sterically crowded complexes **5** and **10**. In **5** the two methyl groups of the dimethylpyridine ligand are inequivalent, and in **10** the methylene hydrogen atoms of the 2-ethylpyridine ligand are diastereotopic, both results inconsistent with rapid ligand dissociation. On the other hand, steric hindrance should inhibit the addition of ligands, and therefore slow substitution by bulky ligands implies an associative mechanism.[2a] A very similar pattern of reactivity has been observed in exchange reactions of substituted pyridine ligands bound to square-planar platinum(II) complexes, which also occur by an associative mechanism.[2,16]

Associative reactions at a tetrahedral metal center might be expected to be similar to S_N2 reactions at tetrahedral carbon. The S_N2 mechanism involves backside attack, in other words attack of the entering group on the tetrahedral face opposite the leaving group, and therefore occurs with inversion of chirality at carbon. Backside attack at the rhenium would similarly invert the configuration at the metal and would thereby effectively exchange the ends of the acetylene ligands. As mentioned above, the acetylene ligands are not fluxional, and the acetylene substituents adjacent to the pyridine ligand give rise to NMR signals that are different from those on the other side of the molecule. The inequivalence of acetylene substituents is maintained under conditions where ligand exchange is rapid, indicating that *the associative exchange reaction does not occur by backside attack.*[17] Substitution proceeds with very high selectivity for retention of configuration; no broadening of the acetylene resonances is observed even under conditions where ligand exchange is very rapid, for example, in solutions of **3** with excess 4-methylpyridine at 80 °C.

Discussion

Associative substitution at tetrahedral centers normally occurs with inversion of stereochemistry, often by backside attack. Displacement with retention of configuration has been observed in phosphorus and silicon chemistry, apparently due either to steric constraints or to the site preferences of different groups in a trigonal-bipyramidal intermediate.[18] The observed retention of configuration in the ligand-exchange reactions at rhenium does not appear to be due to steric factors since the rhenium center is accessible to backside attack, as indicated by the X-ray structure of **2** (Figure 1). The observed stereochemistry is best explained by electronic considerations.

A detailed molecular orbital description of the rhenium oxo–acetylene complexes has been previously presented,[8] and only the conclusions need be summarized here. These complexes are unusual because they are relatively low valent (Re(III), d^4) and still contain a terminal, multiply bonded oxo ligand. A metal–oxygen multiple bond, because of its shortness and strength, plays a critical role in determining the electronic structure and stereochemistry of a complex. Oxo compounds with two d electrons, for example, are almost always diamagnetic and found in square-pyramidal or octahedral structures with approximate fourfold symmetry.[9,13] In d^4 compounds such as the rhenium species dicussed here, there is a strong electronic preference for structures with approximate *threefold* symmetry about the metal–oxygen bond.[8] This is consistent with the structures of **1**, **2**, and **7** as well as the lack of fluxionality in **6** and **7**. The preference for a particular stereochemistry in an oxo complex can be seen in the d orbital splitting pattern. In all cases the d_{z^2}, d_{xz}, and d_{yz} orbitals are strongly antibonding with respect to the metal–oxygen bond (the z axis is taken as coincident with the M–O vector). In fourfold symmetry the $d_{x^2-y^2}$ orbital is also antibonding (toward the ligands in the xy plane), leaving only one nonbonding orbital (d_{xy}); thus stable, diamagnetic d^2 complexes are formed. In C_3 symmetry, however, the $d_{x^2-y^2}$ and d_{xy} orbitals are degenerate and roughly nonbonding so that four d electrons can be accommodated.[8] Note that these electronic preferences depend on the symmetry about the metal–oxygen bond and not on the overall symmetry of the molecule.

This electronic preference appears to be the critical factor in determining the stereochemistry of the substitution reactions. The bias against fourfold symmetry in d^4 oxo complexes strongly destabilizes both square-pyramidal structures with an apical oxo ligand and trigonal-bipyramidal geometries with an equatorial oxo (**A**). Although **A** does not have a strict fourfold axis about

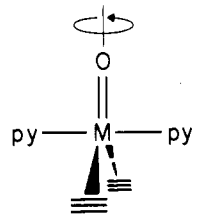

A

the metal–oxygen bond, there are four ligands disposed about this bond; thus the $d_{x^2-y^2}$ orbital has significant σ^* character. Backside attack at the tetrahedral rhenium center in **2–5** or **8–11** (i.e., opposite the leaving group) would form a transition state or intermediate resembling **A**, a trigonal bipyramid with an equatorial oxo ligand, which is a high-energy structure. Thus backside attack does not occur because the resultant five-coordinate geometry would be electronically unfavorable. In contrast, frontside addition of a nucleophile leads to a five-coordinate species which most likely resembles the structure of **7**, very roughly a trigonal bipyramid with an axial oxo ligand. This maintains the preferred threefold symmetry about the metal–oxygen bond.

The bipyridine complexes **6** and **7** are probably excellent models for the transition state or intermediate involved in the pyridine exchange reactions. The stereochemistry is correct, and the rhenium–pyridine bonds are longer than the Re–N bond in **2**, as might be expected for a species along the reaction coordinate for ligand exchange.[19] The stability of **6** and **7** as five-coordinate complexes appears to be due to the strong preference of the bipyridine ligand for bidentate coordination.[20] This strong tendency to chelate apparently overcomes the preference for four-coordination in $ReO(MeC{\equiv}CMe)_2L$ molecules, which is seen

(16) Chottard, J. C.; Mansuy, D.; Bartoli, J. F. *J. Organomet. Chem.* **1974**, *65*, C19–22.

(17) An alternative although unlikely mechanism involves backside attack of a pyridine group with simultaneous rotation of the acetylene ligands, so that in the trigonal-bipyramidal transition state the acetylene ligands (equatorial) lie in the same plane as the (equatorial) Re–O bond. This mechanism, which does not result in the exchange of acetylene substituents, can be ruled out by the exchange reactions of **12**. The methylene hydrogen atoms of the 3-hexyne ligands in **12** are diastereotopic, giving rise to four resonances in the ^1H NMR. The four resonances remain distinct in the presence of excess 4-Mepy when rapid ligand exchange is occurring. This is inconsistent with a backside attack/acetylene rotation mechanism because it would lead to magnetic equivalence of the methylene hydrogens due to the mirror plane present in the transition state.

(18) (a) Westheimer, F. H. *Acc. Chem. Res.* **1968**, *1*, 70–78. (b) Holmes, R. R. *Pentacoordinate Phosphorus*; ACS Monograph 179; American Chemical Society: Washington, DC, 1980; Vol. 2. Luckenbach, R. *Dynamic Stereochemistry of Pentacoordinated Phosphorus and Related Elements*; G. Thieme: Stuttgart, 1973. (c) Corriu, R. J. P.; Guerin, C. *J. Organomet. Chem.* **1980**, *198*, 231–320.

(19) The use of solid-state structures to understand reaction coordinates has been pioneered by Dunitz and co-workers. The structures of **2** and **7** fit well into their models for front- and backside S_N2 displacements at silicon, tin, and cadmium: Burgi, H. B.; Dunitz, J. D. *Acc. Chem. Res.* **1983**, *16*, 153–161. Burgi, H. B. *Inorg. Chem.* **1973**, *12*, 2321–2325. Britton, D.; Dunitz, J. D. *J. Am. Chem. Soc.* **1981**, *103*, 2971–2979. Colvin, E. W.; Beck, A. K.; Bastami, B.; Seebach, D.; Kai, Y.; Dunitz, J. D. *Helv. Chim. Acta* **1980**, *63*, 697–710.

(20) To our knowledge no η^1-bipyridine complexes have been isolated, with the possible exception of "square planar" Pt L_3 (bpy) species. Wernberg, O.; Hazel, A. *J. Chem. Soc., Dalton Trans.* **1980**, 973. Dixon, K. R. *Inorg. Chem.* **1977**, *16*, 2618–2624. Dixon, K. R.; Rattray, A. D. *Can. J. Chem.* **1973**, *51*, 618–623. Bushnell, G. W.; Dixon, K. R.; Khan, M. A. *Can. J. Chem.* **1974**, *52*, 1367–1376. Dholakia, S.; Gillard, R. D.; Widmer, F. L. *Inorg. Chim. Acta* **1982**, *65*, L121–L122. A reported monodentate complex of iridium has recently been shown to be incorrect: Wickramasinghe, W. A.; Bird, P. H.; Serpone, N. *J. Chem. Soc., Chem. Commun.* **1981**, 1284–1286. Nord, G.; Hazell, A. C.; Hazell, R. G.; Farver, O. *Inorg. Chem.* **1983**, *22*, 3429–3434. Spellane, P. J.; Watts, R. J.; Curtis, C. J. *Inorg. Chem.* 4060–4062.

in the monodentate coordination of the acetate ligand in ReO(MeC≡CMe)$_2$[OC(O)Me].[8]

The lack of facile exchange of 2-substituted pyridine ligands can be understood by using the structure of **7** as a model for the intermediate or transition state. There is little room for alkyl groups in the bis-pyridine adduct either between the pyridine ligands or between the oxo group and a pyridine ligand. Even in **7** there is a close contact between the oxo ligand and the hydrogen on C(35) of the bipyridine ligand (2.349 (3) Å).

The five-coordinate bis-pyridine intermediate in the exchange reactions (if there is a discrete intermediate) is probably stereochemically rigid by analogy with the bipyridine complexes **6** and **7**. Although the bidentate nature of the bpy ligand is expected to increase the barrier to pseudorotation, it is unlikely that a bis-pyridine adduct will be fluxional at −90 °C since **7** is rigid on the NMR time scale at 70 °C. Pseudorotation in these species is disfavored because it would have to involve a trigonal-bipyramidal intermediate with an equatorial oxo ligand (A), which is a high-energy structure. The stereochemical rigidity of the five-coordinate intermediate is a significant constraint on the mechanism of ligand exchange.

Associative substitution reactions of compounds of main-group elements, such as silicon and phosphorus, are believed to involve addition and dissociation of nucleophiles through axial positions of a fluxional trigonal-bipyramid intermediate.[18] Pseudorotation is often required to convert the initially formed intermediate into one that leads to products. In the rhenium complexes, addition of a pyridine ligand to the pseudo-axial position "trans" to the oxo forms an intermediate or transition state similar to **6** and **7**. Since this intermediate appears to be rigid on the time scale of ligand exchange, the two pyridine ligands remain distinct. Therefore if the incoming pyridine enters axially, trans to the oxo ligand, the outgoing pyridine must leave from an equatorial position, cis to the oxygen, in order to affect ligand exchange. By the principle of microscopic reversibility,[18a] pyridine ligands must also be able to add cis to the oxo and leave from the trans or axial position. In fact the rate of degenerate ligand exchange that occurs by initial axial attack must be equal to the rate proceeding through equatorial attack.[21] The addition and departure of ligands through an equatorial position of a trigonal bipyramid has been proposed in reactions at four-coordinate silicon[18c] (although the proposal has been the object of criticism[22]).

Thus a detailed picture of the substitution reactions of the rhenium–oxo–acetylene compounds has been developed by using NMR data, molecular orbital analysis, and the X-ray structures of **2** and **7**. The next task is to understand at a more fundamental level why these compounds can react associatively. Addition of ligands to a metal center normally occurs only in coordinatively unsaturated complexes,[5] which would contradict our earlier conclusion that Re(O)I(RC≡CR)$_2$ and [ReO(RC≡CR)$_2$py]$^+$ are 18-electron complexes.[8] The bipyridine complexes **6** and **7**—and the bis-pyridine intermediates or transition states formed in the exchange reactions—therefore seem to be 20-electron species. Twenty-electron compounds are, however, very rare for second- and third-row transition metals.[6] It is possible that the addition of a second pyridine ligand changes the bonding in the complex to reduce the π donation from the oxo or acetylene ligands and thereby reduce the electron count, but there is little evidence of any bonding changes from a comparison of the structures of **2** and **7** or their spectroscopic data. The rhenium–oxygen bonding is clearly similar in the two compounds since the Re–O distances are identical.[23] The rhenium–acetylene interaction appears to be slightly weaker in **7** than in **2** on the basis of differences in bond lengths, but these are much smaller than would be expected if the π donor interaction were eliminated.[24] In addition the ^{13}C NMR chemical shifts, which are a probe of acetylene–metal bonding,[25] are essentially the same in **2**, **3**, **6**, and **7**. Since the bonding in the 16-electron [ReO(RC≡CR)$_2$]$^+$ fragment does not appear to change from **2** to **7**, the ligand-exchange reactions are best described as associative substitution at an 18-electron complex.

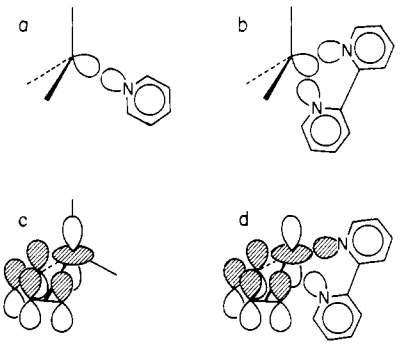

Figure 3. Schematic interaction of [ReO(MeC≡CMe)$_2$]$^+$ fragments with pyridine (a, c) and bipyridine (b, d) ligands.

Associative substitution reactions of coordinatively saturated metal centers have only rarely been observed.[26] They are, however, formally analogous to S_N2 reactions at carbon, which also involve addition of a nucleophile to a saturated center. The lack of associative substitution in most transition-metal compounds is probably due primarily to steric considerations;[26] these likewise often determine the ease of S_N2 processes.[1] The pyridine complexes discussed here have very accessible metal centers because of their low coordination number, which is due to the extensive π donation from the oxo and acetylene ligands.

In the transition state of S_N2 reactions, the entering group binds to the same carbon p orbital as the leaving group in a three-center two-electron bond, and two electrons are in a predominantly nonbonding orbital. The bipyridine complexes **6** and **7** should likewise have three-center bonding. Unusual rhenium–bipyridine bonding is also suggested by the exceptionally long rhenium–nitrogen bond lengths. An orbital description of the rhenium–bipyridine bonding uses the symmetric and antisymmetric com-

(21) The fact that degenerate ligand exchange occurs at equal rates through initial axial or initial equatorial attack can be shown by kinetic analysis using a steady-state approximation on the five-coordinate intermediate. The steady-state treatment is exact in this case because the exchange reactions are at equilibrium and none of the concentrations change with time. Two five-coordinate intermediates must be considered, one formed by axial, the other by equatorial addition; even though these are chemically the same, net exchange only occurs if the ligand lost from the five-coordinate species is different from the one that was added. Note that the two intermediates may be formed at very different rates, but net exchange occurs equally through initial axial or equatorial attack. Definitions: A, four-coordinate species; B_e/B_a, five-coordinate species formed by equatorial/axial addition; and A_e^*/A_a^*, species A that has exchanged through initial equatorial/axial attack

$$L + A_e^* \xleftarrow{k_a} B_e \underset{k_{-e}}{\overset{k_e}{\rightleftharpoons}} A + L \underset{k_{-a}}{\overset{k_a}{\rightleftharpoons}} B_a \xrightarrow{k_{-e}} A_a^* + L$$

After steady state on $[B_e]$ and $[B_a]$, $d[A_e^*]/dt = [k_{-a}k_e/(k_{-e} + k_{-a})][A][L]$ and $d[A_a^*]/dt = [k_{-e}k_a/(k_{-e} + k_{-a})][A][L]$. Since the equilibrium constant $K(A + L \rightleftharpoons B)$ is the same for B_e and B_a, $K = k_a/k_{-a} = k_e/k_{-e}$, or $k_{-a}k_e = k_{-e}k_a$; therefore $d[A_e^*]/dt = d[A_a^*]/dt$.

(22) Holmes, R. R.; Day, R. O.; Chandrasekhar, V.; Harland, J. J.; Holmes, J. M. *Inorg. Chem.* **1985**, *24*, 2016–2020.

(23) Although the Re–O bond distances are the same in **2** and **7**, the stretching frequencies are significantly different (**2**, **3**: 969, 673 cm^{-1}; **6**, **7**: 950, 955 cm^{-1}). This shift to lower frequencies often occurs on adding a trans ligand to a square-pyramidal oxo complex but is thought to have little influence on metal–oxygen bonding. See: Collin, R. J.; Griffith, W. P.; Pawson, D. *J. Mol. Struct.* **1973**, *19*, 531–544. Jezowska-Trezebiatowska, B.; Hanuza, J. *J. Mol. Struct.* **1973**, *19*, 109–142. See also ref 9a.

(24) The structural parameters most sensitive to changes in the metal–acetylene bonding interaction are the metal–carbon distances. The rhenium–carbon distances in **1**, **2**, and **7** (average 2.051, 2.047, and 2.059 Å) are in between the values for the two-electron and four-electron donor acetylene complexes CpRe(CO)$_2$(PhC≡CPh) (average 2.189 (10) Å) and ReCl$_3$(PMePh$_2$)$_2$(MeC≡CMe) (average 1.957 (5) Å): Einstein, F. W. B.; Tyers, K. G.; Sutton, D. *Organometallics* **1985**, *48*, 489–493. Tulip, T., unpublished results. A similar comparison of tungsten compounds also concludes that large (~0.1 Å) changes in metal–carbon distances accompany significant changes in metal–acetylene bonding: Ricard, L.; Weiss, R.; Newton, W. E.; Chen, G. J.-J.; McDonald, J. W. *J. Am. Chem. Soc.* **1978**, *100*, 1318–1320. See also ref 25.

(25) Templeton, J. L.; Ward, B. C. *J. Am. Chem. Soc.* **1980**, *102*, 3288–3290. Templeton, J. L.; Ward, B. C.; Chen, G. J.-J.; McDonald, J. W.; Newton, W. E. *Inorg. Chem.* **1981**, *20*, 1248–1253.

(26) Graham, J. R.; Angelici, R. J. *Inorg. Chem.* **1967**, *6*, 2082–2085. Reference 2.a, p. 98.

binations of the bipyridine lone pairs, which are isolobal[27] with the filled π orbitals of an acetylene ligand oriented perpendicular to the bipyridine plane.[8] The symmetrical combination of the bipyridine lone pairs bonds with the rhenium in a three-center two-electron interaction analogous to the two-center two-electron interaction of a single pyridine ligand (Figure 3a,b). The antisymmetric combination of lone pairs is oriented to overlap well with the rhenium d_{z^2} orbital, as are the acetylene π donor orbitals (Figure 3d). In the pyridine complex there is already substantial bonding between the acetylene ligands and the d_{z^2} orbital (Figure 3c). This acetylene π donation to rhenium seems to be only slightly diminished in the bipyridine complex, as evidenced by the structural and spectroscopic data described above, so the bipyridine ligand seems to play only a minor role in this interaction (Figure 3d). Similar arguments indicate that there is at most a weak interaction between the bipyridine ligand and the rhenium d_{xz} orbital, which is engaged in rhenium–oxygen bonding. Thus bipyridine seems to be acting principally as a two-electron donor to rhenium via the three-center interaction described above. The very long rhenium–nitrogen distances appear to be due to the bipyridine ligand being bound to rhenium primarily with one pair of electrons, so that each Re–N bond is roughly of order one-half. This orbital analysis can also rationalize the unusual coordination geometry of **7**, which may best be described as a tetrahedron in which the bipyridine ligand occupies one site.

Conclusions

The rhenium–oxo–bis(acetylene)–pyridine complexes $[ReO(RC{\equiv}CR')_2L]^+$ undergo a very rapid ligand-exchange reaction with free pyridine in solution, unless the pyridine is substituted at the 2-position. The fact that sterically hindered ligands undergo less facile exchange indicates an associative mechanism. NMR studies show that ligand substitution proceeds with retention of stereochemistry and not by backside attack at the tetrahedral rhenium center. Addition apparently occurs cis to the leaving ligand, forming a nonfluxional five-coordinate intermediate or transition state that probably resembles the structure of the isolated bipyridine adduct **7**. The unusual preference for retention of configuration is due to the electronic influence of the rhenium–oxygen multiple bond. The rhenium–pyridine complexes are best described as 18-electron species; the ligand-exchange reactions therefore involve attack at a coordinatively saturated center. The exchange reactions appear to be similar to S_N2 reactions at saturated carbon centers, except for the difference in stereochemistry.

Experimental Section

Syntheses were performed in a continuous nitrogen flow glovebox, by standard vacuum-line techniques, or on the bench-top. All solvents were deoxygenated and dried by standard methods. Compounds **1**, **2**, **6**, **8**, **11**, and $Re(O)I(EtC{\equiv}CEt)_2$ have been previously reported.[8] NMR spectra were obtained with Nicolet NT200, NT300, NT360, QE300, Varian FT80, Bruker CXP200, WM400, and WM500 spectrometers. NMR spectra of **2**–**12** were taken in CD_2Cl_2 at ambient temperatures; chemical shifts are reported in ppm downfield from Me_4Si, and coupling constants are reported in Hz: δ (multiplicity, J value). IR spectra were obtained on Nujol mulls with Perkin-Elmer 283B and 983G spectrophotomers. Elemental analyses were performed by Galbraith Labs. Pyridines were purchased from Aldrich and were distilled before use. $AgSbF_6$ (Aldrich) was used as received, although it contains water, which interferes with the syntheses of **5** and **10**.

$[ReO(MeC{\equiv}CMe)_2(4\text{-Mepy})]SbF_6$ (3). A solution of $AgSbF_6$ (70 mg, 0.20 mmol) in 5 mL of CH_2Cl_2 at ambient temperatures was added dropwise over a 5-min period to a stirred, −78 °C solution of **1** (87 mg, 0.20 mmol) and 4-methylpyridine (18 mg, 0.20 mmol) in 5 mL of CH_2Cl_2. After the flask was allowed to warm to room temperature, the solution was filtered, stripped to dryness, and rinsed several times with diethyl ether, giving 80 mg of pale-green **3** (63%): IR 1638 (4-Mepy), 1247, 1212, 1151, 1067, 1041, 972 st (ReO), 871, 818, 768, 737, 625 st (SbF_6) cm^{-1}; ^1H NMR 2.34 (q, 1), 3.24 (q, 1) ($CH_3C{\equiv}CCH_3$), 2.69 (s), 7.72 (d, 7), 7.98 (d, 6) (4-Mepy); ^{13}C NMR 145.97 (s), 143.45 (s) ($CH_3C{\equiv}CCH_3$), 16.70 (q, 132), 9.94 (q, 132) ($CH_3C{\equiv}CCH_3$), 21.87 (q, 133) ($CH_3C_5H_4N$), 150.55 (d, 185) (C^2, C^6), 130.35 (d, 169) (C^3, C^5), 155.89 (s, C^4). Anal. Calcd for $C_{14}H_{19}NOReSbF_6$: C, 26.31; H, 3.00. Found: C, 26.11; H, 3.07.

$[ReO(MeC{\equiv}CMe)_2(2\text{-Mepy})]SbF_6$ (4). Following the procedure for **3**, 87 mg of **1**, 70 mg of $AgSbF_6$, and 18.6 mg of 2-methylpyridine (all 0.20 mmol) gave 92 mg of pale-green **4** (73%): IR 1628 (2-Mepy), 1315, 1158, 1125, 1042, 977 st (ReO), 912, 773, 722, 659 st (SbF_6) cm^{-1}; ^1H NMR 2.26 (q, 1), 3.29 (q, 1) ($CH_3C{\equiv}CCH_3$), 2.97 (s), 6.42 (d, 6), 7.50 (td, 7, 1), 7.99 (d, 8), 8.11 (td, 7, 1) (2-Mepy); ^{13}C NMR 141.32 (s), 145.75 (s) ($CH_3C{\equiv}CCH_3$), 16.73 (q, 132), 9.92 (q, 132) ($CH_3C{\equiv}CCH_3$), 28.31 (q, 130) ($CH_3C_5H_4N$), 157.06 (s) (C^2), 129.75 (d, 176) (C^3), 142.07 (d, 169) (C^4), 125.95 (d, 177) (C^5), 148.75 (d, 186) (C^6). Anal. Calcd for $C_{14}H_{19}NOReSbF_6$: C, 26.31; H, 3.00. Found: C, 26.27; H, 2.94.

$[ReO(MeC{\equiv}CMe)_2(2,6\text{-}Me_2py)]SbF_6$ (5). A 10 °C solution of $AgSbF_6$ (80 mg, 0.23 mmol) in 2 mL of CH_2Cl_2 was added dropwise to a stirred, −40 °C solution of **1** (100 mg, 0.23 mmol) and 2,6-Me_2py (26.0 μL, 0.23 mmol) in 2 mL of CH_2Cl_2 in a drybox. The solution was stirred for 10 min, filtered, and reduced to 2 mL; addition of hexane yielded 72 mg of tan **5** (48%): ^1H NMR 2.35 (q, 1), 3.32 (q, 1) ($CH_3C{\equiv}CCH_3$), 0.95 (s), 2.94 (s), 7.42 (d, 8), 7.60 (d, 6), 8.28 (t, 8) (Me_2py). Compound **5** is usually contaminated with $[Me_2pyH]^+[SbF_6]^-$ (the proton arising from H_2O in the $AgSbF_6$) and has not been isolated in pure form.

$[ReO(MeC{\equiv}CMe)_2(4,4'\text{-}Me_2bpy)]SbF_6$ (7). Following the procedure for **5**, 300 mg of **1** (0.69 mmol), 234 mg of $AgSbF_6$ (0.68 mmol), and 126 mg of 4,4′-dimethylbipyridine (0.68 mmol) were stirred for 1 h, filtered, and then precipitated with hexane, yielding 310 mg of pale-green **7** (61%): IR 1618, 1579 (4,4′-Me_2bpy), 1304, 1244, 1223, 1154, 1042, 1015, 951 st (ReO), 929, 843, 828, 655 st (SbF_6) cm^{-1}; ^1H NMR 2.07 (q, 1), 3.23 (q, 1) ($CH_3C{\equiv}CCH_3$), 2.56 (s), 2.74 (s), 5.89 (d, 6), 7.13 (d, 6), 7.55 (d, 6), 8.28 (s), 8.46 (s), 8.66 (d, 6) (4,4′-Me_2bpy); ^{13}C NMR 147.21 (s), 138.77 (s) $CH_3C{\equiv}CCH_3$), 16.72 (q, 130), 11.82 (q, 130) ($CH_3C{\equiv}CCH_3$), 21.15 (q, 129), 20.79 (q, 129) ((CH_3)$_2$bpy); 150.86 (s), 147.99 (s) (C^2, $C^{2'}$), 123.93 (d, 166), 124.32 (d, 166) (C^3, $C^{3'}$), 153.13 (s), 155.33 (s) (C^4, $C^{4'}$), 127.26 (d, 167), 128.19 (d, 169) (C^5, $C^{5'}$), 144.77 (d, 182), 151.58 (d, 186) (C^6, $C^{6'}$).

$[ReO(Me_3CC{\equiv}CH)_2(4\text{-Etpy})]SbF_6$ (9). Following the general procedure for **3** (except the solution was heated for 10 min with a warm water bath (40 °C) prior to filtration of AgI solids), 40 mg of $ReO(Me_3CC{\equiv}CH)_2I$, 28 mg of $AgSbF_6$, and 8.7 mg of 4-ethylpyridine (all 0.08 mmol) afforded 45 mg of cream-colored **9** (81%): IR 1695 (w), 1640, 1622, 1234, 1205, 1064, 1051, 1036, 981 st (ReO), 941, 906, 837, 777, 722, 648 st (SbF_6); ^1H NMR 1.12 (s), 1.67 (s) ((CH_3)$_3$CC≡CH), 9.03 (s), 10.97 (s) ($Me_3CC{\equiv}CH$), 1.39 (t, 8), 2.99 (q, 8), 7.76 (d, 5), 8.36 (d, 6) (4-Etpy); $^{13}C\{^1H\}$ NMR 128.76, 130.99 ($Me_3CC{\equiv}CH$), 38.79, 40.05 ($Me_3CC{\equiv}CH$); 32.34 ((CH_3)$_3$CC≡CH), 14.92, 25.72 (CH_3CH_2py); 129.78 (Etpy) (C^3, C^5), 142.20, 153.17, 163.36, 166.76 (EtC_5H_4N, $Me_3CC{\equiv}CH$).

$[ReO(Me_3CC{\equiv}CH)_2(2\text{-Etpy})]SbF_6$ (10). Following the procedure for **5**, 50 mg of $Re(O)I(Me_3CC{\equiv}CH)_2$, 35 mg of $AgSbF_6$, and 10.7 mg of 2-ethylpyridine (all 0.10 mmol) gave 48 mg of cream-colored **10** (71%): ^1H NMR 1.08 (s), 1.70 (s) ((CH_3)$_3$CC≡CH), 8.87 (s), 10.85 (s) ($Me_3CC{\equiv}CH$), 1.61 (t, 8) ($CH_3CH_2C_5H_4N$), 3.29 (dq, 16, 8), 3.45 (dq, 16, 8) ($MeCHH'C_5H_4N$), 6.34 (d, 6), 7.48 (td, 8, 1), 8.02 (d, 6), 8.16 (td, 8, 1) (EtC_5H_4N). Compound **10** is usually contaminated with $[EtpyH]^+[SbF_6]^-$ (the proton arising from H_2O in the $AgSbF_6$) and has not been isolated in pure form.

$[ReO(EtC{\equiv}CEt)_2(4\text{-Mepy})]SbF_6$ (12). Following the procedure for **3** (except that the product was isolated by precipitation with pentane), $AgSbF_6$ (52 mg, 0.15 mmol), $Re(O)I(EtC{\equiv}CEt)_2$ (75 mg, 0.15 mmol), and 4-methylpyridine (14 mg, 0.15 mmol) yielded 45 mg of tan **12** (64%): IR 1623, 1218, 1150, 1065, 980 st (ReO), 822, 722, 660 st (SbF_6) cm^{-1}; ^1H NMR 1.20 (t, 8), 1.54 (t, 8) ($CH_3CH_2C{\equiv}CCH_2CH_3$), 2.44 (dq, 16, 8), 2.78 (dq, 16, 8), 3.39 (dq, 16, 8), 3.71 (dq, 16, 8) ($CH_3CHH'C{\equiv}CCHH'CH_3$), 2.69 (s, $CH_3C_5H_4N$), 7.73 (d, 6), 8.10 (d, 6) ($CH_3C_5H_4N$); $^{13}C\{^1H\}$ NMR 147.83, 150.36 ($EtC{\equiv}CEt$), 20.64, 26.80 ($CH_3CH_2C{\equiv}CCH_2CH_3$), 15.30 ($CH_3CH_2C{\equiv}CCH_2CH_3$), 23.02 ($CH_3C_5H_4N$), 151.71 ($C^2$, C^6), 131.30 (C^3, C^5), 156.95 (C^4). Anal. Calcd for $C_{18}H_{27}NOReSbF_6$: C, 31.09; H, 3.91; N, 2.01. Found: C, 31.19; H, 3.86; N, 2.60.

Low-temperature NMR spectra were obtained with a Nicolet NT300. The methyl resonances for **3** (0.067 M in CD_2Cl_2) and 4-methylpyridine (0.064 M) were not coalesced at −90 °C, which places an upper limit on the lifetime for exchange of $\tau < 4.4$ ms[28] and a lower limit on the bimolecular rate constant of $k > 1.7 \times 10^3$ M^{-1} s^{-1}.[29] The high-temperature spectra of **4** (0.022 M in CD_2Cl_2) and 2-methylpyridine (0.035 M), obtained with a Bruker CXP200, showed coalescence of the methyl resonances at 62°C, which can be converted to a bimolecular rate con-

(27) Hoffman, R. *Angew. Chem., Int. Ed. Engl.* **1982**, *21*, 711–724.

(28) Sandström, J. *Dynamic NMR Spectroscopy*; Academic: New York, 1982; p 79.

Table IV. Summary of X-ray Diffraction Data

	[ReO(MeC≡CMe)$_2$py]SbF$_6$ (**2**)	[ReO(MeC≡CMe)$_2$(4,4′-Me$_2$bpy)]SbF$_6$ (**7**)
formula	$C_{13}H_{17}F_6ONReSb$	$C_{20}H_{24}F_6N_2OReSb$
fw	625.27	730.37
space group	$P\bar{1}$ (no. 2)	$P2_1/c$ (no. 14)
a, Å	10.482 (1)	7.872 (1)
b, Å	12.117 (2)	21.735 (3)
c, Å	7.880 (1)	13.492 (2)
α, deg	105.34 (1)	90.0
β, deg	108.03 (1)	100.70 (1)
γ, deg	99.05 (1)	90.0
V, Å^3	886 (1)	2268 (1)
Z	2	4
ρ(calcd), g cm^{-3}	2.343	2.14
crystal dimensions, mm	0.29 × 0.19 × 0.34	0.17 × 0.21 × 0.35
temp, °C	−100	−100
radiation	Mo Kα[a]	Mo Kα[a]
μ, cm^{-1}	85.11	66.66
2θ limits, deg	4.2–55.0	4.0–55.0
transmission factors	0.13–0.25	0.74–1.00
total no. of unique observations	4393	5572
data[b]	3752	3926
final no. of variables	244	280
R	0.020	0.026
R_w	0.027	0.028

[a] 0.71069 Å, from graphite monochromator. [b] $F_o^2 > 3\sigma(F_o^2)$.

stant[28,29] $k = 5.1\ (\pm 0.5) \times 10^3$ M^{-1} s^{-1} at this temperature.

X-ray Data Collection, Structure Solutions, and Refinements. [ReO(MeC≡CMe)$_2$py]SbF$_6$ (2). Crystals of compound **2** were grown by slowly cooling a methylene chloride solution. A suitable crystal was encapsulated in a glass capillary under an atmosphere of N_2. The crystal was then placed on a Syntex R3 diffractometer and cooled at −100 °C. After the cell and space group had been determined (Table IV), the unit-cell parameters were refined on the basis of 23 computer-centered reflections.

The ω-scan technique was used for intensity data collection (variable scan rate 2.0–9.8° min^{-1}, 1.1° range). Three standard reflections, monitored throughout the irradiation, showed negligible variation in intensity. The data were corrected for absorption by using the DIFABS method and processed by using counting statistics and a p value of 0.03 to derive standard deviations.[30,31]

Initial phases were obtained via an automated Patterson technique, and the solution was refined by the usual combination of Fourier syntheses and least-squares refinements with a program package assembled by J.C.C. In the least-squares refinements, the function minimized was $\sum w(|F_o| - |F_c|)^2$, where $|F_c|$ and $|F_o|$ are the observed and calculated structure amplitudes and where $w = \sigma^{-2}(F_o)$. The atomic scattering factors and anomalous dispersion terms were taken from the standard compilation.[32] Hydrogen atoms were located, placed in idealized positions, and included as a fixed contribution in the final refinement cycles. With $R = 0.023$, disorder in the SbF_6 anion was observed. Multiplicity refinements yielded the final results, in which the equatorial F atoms [F(3, 4, 5, 6)] each occupy two sites, with 20% weighting in the F′ positions. The final positional and isotropic thermal parameters are listed in Table I, with the anisotropic thermal parameters and hydrogen atom positions (Table V) available as supplementary material, as are observed and calculated structure factor amplitudes (Table VI).

[ReO(MeC≡CMe)$_2$(Me$_2$bpy)]SbF$_6$ (7). Crystals of complex **7** were grown and manipulated as above. Unit-cell parameters (Table IV) were obtained on the basis of 46 reflections. Data were collected and processed as above, except that the scan rate was 4.0–10.0° min^{-1} and the p value was 0.02. The solution and refinement of the structure were carried out by using local modifications of the SDP-Plus program series supplied by the Nonius-Enraf Corp. Positional and isotropic thermal parameters of the atoms of complex **7** are listed in Table II. Anisotropic thermal parameters (Table VII), hydrogen atom positions (Table VII), and a listing of observed and calculated structure factor amplitudes (Table VIII) are available as supplementary material. Final values for agreement indices are listed in Table IV.

Acknowledgment. We would like to thank D. L. Thorn for his invaluable suggestions and advice. The skilled technical assistance of G. Barkley and L. Lardear is gratefully appreciated. We would also like to acknowledge the Danforth–Compton Foundation for a fellowship to E.V. This work was supported in part by an M. J. Murdock Charitable Trust Grant of the Research Corp.

Supplementary Material Available: Tables listing anisotropic thermal parameters and hydrogen atomic coordinates for **2** and **7** (5 pages); tables of calculated and observed structure factors (29 pages). Ordering information is given on any current masthead page.

(29) Jackman, L. M.; Cotton, F. A. *Dynamic Nuclear Magnetic Resonance Spectroscopy*; Academic: New York, 1975; p 623.

(30) Walker, N.; Stuart, D. *Acta Crystallogr., Sect. A: Found. Crystallogr.* **1983**, *A3*, 158–166.

(31) Corfield, P. W. R.; Doedens, R. J.; Ibers, J. A. *Inorg. Chem.* **1967**, *6*, 197–204.

(32) *International Tables for X-ray Crystallography*: Kynoch: Birmingham, England, 1974; Vol. IV, Tables 2–2B, p 2.3.1.